1

2 **Running head:** AtNRAMP3 and AtNRAMP4 function in vacuolar Mn export (53

3 characters)

4

5 **Corresponding author:**

6 Sébastien Thomine

7 Institut des Sciences du Végétal, CNRS, Avenue de la Terrasse, 91198 Gif-sur-

8 Yvette, France

9 Tel : +33 1 69 82 37 93

10 thomine@isv.cnrs-gif.fr

11

12

13

14

15 **Journal research area**

16 Environmental Stress and Adaptation

17

1 **Title:** Export of vacuolar manganese by AtNRAMP3 and AtNRAMP4 is required for

2 optimal photosynthesis and growth under manganese deficiency

3

4

5

6 **Authors:**

7 Viviane Lanquar[1]*, Magali Schnell Ramos[1], Françoise Lelièvre[1], Hélène Barbier-

8 Brygoo[1], Anja Krieger-Liszkay[2], Ute Krämer[3], Sébastien Thomine[1]†

9 1 Institut des Sciences du Végétal, CNRS, Avenue de la Terrasse, 91198 Gif-sur-

10 Yvette, France

11 2 Service de Bioénergétique Biologie Structurale et Mécanismes (SB2SM), iBiTec-S,

12 CEA Saclay, 91191Gif-sur-Yvette, France

13 3 University of Heidelberg, BIOQUANT 23, Im Neuenheimer Feld 267, D-69120

14 Heidelberg, Germany

15

6

* present address: Carnegie Institution for Science, Department of Plant Biology, 260 Panama Street, Stanford CA 94 305, USA

9

†For correspondence: thomine@isv.cnrs-gif.fr

11

12

3

1 **Abstract:**

2 **(201 words)**

3 Manganese is an essential element, acting as cofactor in numerous enzymes. In

4 particular, a Mn cluster is indispensable for the function of the oxygen evolving

5 complex of photosystem II. Metal transporters of the natural resistance associated

6 macrophage protein (NRAMP) family have the ability to transport both iron and

7 manganese. AtNRAMP3 and AtNRAMP4 are required for iron mobilization in

8 germinating seeds. The results reported here show that, in adult *Arabidopsis thaliana*

9 plants, AtNRAMP3 and AtNRAMP4 have an important role in Mn homeostasis.

10 Vacuolar Mn accumulation in mesophyll cells of rosette leaves of adult

11 *nramp3nramp4* double mutant plants was dramatically increased when compared to

12 wild type. This suggests that a considerable proportion of the cellular Mn pool passes

13 through the vacuole and is retrieved in an AtNRAMP3/AtNRAMP4-dependent

14 manner. The impaired Mn release from mesophyll vacuoles of *nramp3nramp4* double

15 mutant plants is associated with reduced growth under Mn deficiency. However, leaf

16 AtNRAMP3 and AtNRAMP4 protein levels are unaffected by Mn supply. Under Mn

17 deficiency, *namp3nramp4* plants contain less functional photosystem II than the wild

18 type. These data are consistent with a shortage of Mn to produce functional

19 photosystem II, whereas mitochondrial Mn dependent superoxide dismutase (SOD)

20 activity is maintained under Mn deficiency in both genotypes. The results presented

21 here suggest an important role for AtNRAMP3/AtNRAMP4-dependent Mn transit

22 through the vacuole prior to the import into chloroplasts of mesophyll cells.

23

24 **Introduction**

25 The catalytic centers of numerous enzymes rely on the ability of some transition

26 metals to undergo changes in their redox state. Although Mn is involved as a cofactor

27 in a range of additional biochemical pathways, the primary effect of Mn deficiency in

28 photosynthetic organisms is a drop in photosynthetic activity (Marschner, 1995). The

29 process of water splitting and oxygen evolution by photosystem II (PS II), which is a

30 central component of oxygenic photosynthesis, requires a tetra-Mn cluster.

31 In plants, few of the mechanisms that enable the uptake, distribution, and storage of

32 Mn have been characterized at the molecular level. Hyperpolarisation-activated Ca^{2+}

33 channels and members of the ZIP family have been proposed as pathways for Mn

34 uptake in roots (Korshunova et al., 1999; Vert et al., 2002; White et al., 2002; Pedas

4

1 et al., 2008). However, to our knowledge, no transporter specifically functioning in Mn

2 uptake from soils has been reported in the root plasma membrane.

3 Most of the current knowledge on Mn compartmentation in plant cells comes from the

4 analysis of the mechanisms of tolerance to Mn excess. Indeed, when accumulated in

5 excess, Mn can be toxic and has been proposed to be sequestered in vacuoles and

6 Golgi vesicles under these conditions (Marschner, 1995; Pittman, 2005). The

7 analysis of the molecular mechanisms of Mn tolerance in *Stylosanthes hamata*, a

8 tropical legume tolerant to high Mn led to the cloning of the Mn specific transport

9 protein ShMTP8 (Delhaize et al., 2003). When expressed in Arabidopsis, ShMTP8 is

10 targeted to the vacuolar membrane and confers Mn tolerance by mediating the

11 sequestration of excess Mn in this compartment. In Arabidopsis, several pathways

12 for Mn import into the vacuole have been identified. AtCAX2 and AtCAX4 Ca^{2+}/H^+

13 antiporters are able to transport Mn into the vacuole (Hirschi et al., 2000; Pittman et

14 al., 2004; Koren'kov et al., 2006). In addition, AtVIT1 increases the Mn content of the

15 vacuoles when expressed in yeast (Kim et al., 2006). AtVIT1 is thus a good

16 candidate to mediate Mn import into vacuoles. Recently, the functional analysis of

17 AtMTP11 and PtMTP11, the homologues of ShMTP8 in Arabidopsis and poplar,

18 suggested the existence of an alternative pathway for Mn detoxification by vesicle-

19 mediated transport of this metal (Delhaize et al., 2007; Peiter et al., 2007). In

20 addition, over expression of the Mn transporting P_{2A}-type ATPase, *AtECA1*, localized

21 to the endoplasmic reticulum, increased Mn tolerance (Wu et al., 2002). Whether the

22 vacuole represents an important site for the storage of Mn in plants grown under

23 normal conditions is currently unknown. Moreover, little is known about the

24 mechanisms involved in plant tolerance to Mn deficiency.

25 Recent work on barley confirmed an important decrease in the abundance of

26 functional photosystem II under Mn deficiency and revealed differences in the

27 fluorescence induction kinetics and state transitions between Mn efficient and

28 inefficient genotypes (Husted et al., 2009). In barley, Mn deficiency also leads to

29 increased water loss, likely through alteration of the leaf cuticle (Hebbern et al.,

30 2009). Interestingly, in *C. reinhardtii*, another photosynthetic organism, in addition to

31 causing a decrease in functional PS II abundance, Mn deficiency also impairs Mn

32 dependent superoxide dismutase activity, leading to an increased sensitivity to

33 oxidative stress (Allen et al., 2007). The cellular pathways for Mn transport and use

34 under Mn deficient conditions are mostly unknown. A recent study on the Mn

5

transporting P$_{2A}$-type ATPase, *AtECA3*, localized to the Golgi apparatus, demonstrated the importance of Mn import into the Golgi apparatus under Mn deficiency (Mills et al., 2008).

NRAMPs represent another protein family likely to be involved in Mn transport in plants. Most NRAMP proteins characterized so far are able to transport a broad range of metals: Fe^{2+}, Mn^{2+}, Zn^{2+}, Cd^{2+} [for review: (Colangelo and Guerinot, 2006; Nevo and Nelson, 2006)]. In bacteria, NRAMP homologues, MntH, function primarily as cellular Mn uptake transporters (Makui et al., 2000). Moreover, *MntH* gene expression is regulated at the transcriptional level through MntR, a Mn-sensing regulatory protein (Que and Helmann, 2000; Patzer and Hantke, 2001). In *C. reinhardtii, NRAMP1* is up-regulated upon Mn deprivation (Allen et al., 2007). In yeast, NRAMP homologues, Smf1p and Smf2p, are involved in Mn uptake and recycling. They are co-regulated at the post-translational level by this metal (Liu and Culotta, 1999; Portnoy et al., 2000). The disruption of *SMF2* leads to the loss of activity of the mitochondrial Mn superoxide dismutase (SOD) and of Golgi Mn-dependent enzymes (Luk and Culotta, 2001).

In Arabidopsis, six members of the NRAMP family have been identified. Heterologous expression of the *AtNRAMP1, 3* and *4* cDNAs in yeast mutants deficient for metal uptake, indicated that these proteins are able to transport Fe, Mn and Cd (Curie et al., 2000; Thomine et al., 2000). AtNRAMP3-GFP and AtNRAMP4-GFP fusion proteins are targeted to the vacuolar membrane (Thomine et al., 2003; Lanquar et al., 2005). In addition, AtNRAMP4 was identified in the vacuolar proteome of Arabidopsis mesophyll cells (Carter et al., 2004). *AtNRAMP3* and *AtNRAMP4* are strongly expressed during the early stages of germination and the *nramp3nramp4* double mutant displays a strong chlorotic phenotype when seeds are germinated in the absence of Fe supply in the medium (Lanquar et al., 2005). It was thus proposed that AtNRAMP3 and AtNRAMP4 play redundant roles in export of Fe from the vacuole during seed germination. In the present study, a detailed examination of the *nramp3nramp4* double mutant adult plants indicated that AtNRAMP3 and AtNRAMP4 crucially contribute to Mn homeostasis. AtNRAMP3 and AtNRAMP4 are required for Mn mobilization from the vacuole of mesophyll cells in adult plants. As a consequence, *nramp3nramp4* over-accumulate Mn in vacuoles under standard growth conditions, and *nramp3nramp4* growth is strongly impaired under Mn deficiency. This growth phenotype is associated with a decrease in the number of

6

1 functional PSII attributable to a shortage of Mn clusters, whereas mitochondrial Mn

2 SOD activity is maintained. The results presented show that AtNRAMP3 and

3 AtNRAMP4 play a major role in the export of vacuolar Mn in photosynthetic tissues of

4 adult plants. These results highlight the importance of Mn transit through vacuoles en

5 route to its main usage site in chloroplasts.

6

7 Results

8 **AtNRAMP3 and AtNRAMP4 are involved in Mn retrieval from the vacuole of**

9 **mesophyll cells**

10 To gain insight into the function of AtNRAMP3 and AtNRAMP4 in adult plants, the

11 consequences of their absence were investigated in mesophyll cells from plants

12 grown on soil for 6 weeks.

13 Intact mesophyll protoplasts were released from rosette leaves and subsequently,

14 the mesophyll protoplast preparation was subjected to gentle lysis and intact

15 vacuoles were recovered. Microscopic observation of the protoplast preparation

16 revealed that only mesophyll protoplasts were present, no other cell types could be

17 recognized and that the vacuole preparation was of high purity. Furthermore,

18 vacuolar pyrophosphatase (V-PPase), a vacuolar membrane protein, was enriched in

19 the vacuole preparation in comparison to the protoplast from which they were

20 extracted (Figure 1A), whereas E37, a chloroplast envelope protein was not detected

21 (data not shown) (Ferro et al., 2002).

22 AtNRAMP3 and AtNRAMP4 protein levels were examined in leaves, mesophyll

23 protoplasts and vacuoles by immunoblot using isoform specific antibodies (Figure

24 S1) (Lanquar et al., 2005). In *nramp3nramp4* leaves, protoplasts or vacuoles, no

25 signal corresponding to AtNRAMP3 or AtNRAMP4 was detected (Figure 1A),

26 confirming the absence of both proteins. In wild-type plants, AtNRAMP3 and

27 AtNRAMP4 were detected in leaves and in mesophyll protoplasts. There was only a

28 weak signal for AtNRAMP3 in mesophyll protoplasts. This indicates that AtNRAMP3

29 may be more abundant in other leaf tissues, such as the vasculature, than in

30 mesophyll, in agreement with *AtNRAMP3* expression pattern (Thomine et al., 2003).

31 In mesophyll vacuoles, the signals corresponding to AtNRAMP3 and AtNRAMP4

32 were about 20 times stronger than in mesophyll protoplasts, indicating an enrichment

33 of these two membrane proteins (Figure 1A). These results indicate that both

34 AtNRAMP3 and AtNRAMP4 are localized in the vacuolar membrane of mesophyll

7

cells of adult leaves as previously reported in other cell types (Thomine et al., 2003; Lanquar et al., 2005).

To investigate the functions of AtNRAMP3 and AtNRAMP4 in mesophyll cells, the metal concentrations were measured by ICP-AES in leaf tissues, mesophyll protoplasts and mesophyll vacuoles of wild-type and *nramp3nramp4* plants grown on soil. The concentrations of iron, manganese and zinc, three possible substrates of NRAMP3 and NRAMP4, were similar in *nramp3nramp4* and wild-type leaves (Figure 1B). This result is consistent with published data on younger seedlings (Lanquar et al., 2005). Similarly, no statistically significant differences were observed between metal contents of *nramp3nramp4* and wild-type mesophyll protoplasts for Fe, or Zn (Figure 1B). By contrast, protoplasts isolated from *nramp3nramp4* plants contained 2.1 to 2.8 more Mn than wild-type protoplasts (Figure 1B). Furthermore, analysis of *nramp3nramp4* vacuoles revealed that they contained between 6.5 and 56 times more Mn than wild-type vacuoles (Figure 1B). An additional experiment employing an independent *nramp3nramp4* double knockout mutant in the Columbia accession confirmed the strongly increased vacuolar Mn content in *nramp3nramp4* double mutants when compared to the wild type (Ravet et al., 2009b). Microscopic observations did not show any size difference between wild-type and *nramp3nramp4* double mutant vacuoles. Furthermore, no statistically significant difference in vacuolar contents of Fe or Zn was detected between the double mutant and the wild type.

These results show that the loss of AtNRAMP3 and AtNRAMP4 proteins greatly enhances the sequestration of Mn in mesophyll vacuoles, while in wild-type plants, AtNRAMP3 and AtNRAMP4 continuously mediate the retrieval of Mn from the vacuole. Furthermore, these results suggest that net Mn storage in the vacuole of mesophyll cells is minor in wild-type *A. thaliana* under normal growth conditions (about 10% of protoplast Mn), but that a substantial proportion of cellular Mn transits through the vacuole.

Adult *nramp3nramp4* plants display a conditional growth defect under Mn deficiency

The results of this study indicate that in *nramp3nramp4* mesophyll cells, Mn sequestration in the vacuole is strongly increased. To test whether this alteration in intracellular Mn distribution is associated with a defect in plant growth, plants were grown on perlite and watered either with a control Mn-sufficient nutrient solution

8

containing 5 µM Mn (C) or with a nutrient solution lacking Mn (Mn-deficient conditions, - Mn). After 9.5 weeks of growth, the biomass of *nramp3nramp4*, *nramp3* and *nramp4* mutant rosettes grown under control conditions was not significantly different from that of wild-type plants (Figure 2A, C, D and Table I). The rosettes of adult *nramp3nramp4* mutant appeared smaller because their leaves were curled: the leaf margins grow towards the abaxial side of the leaf (Figure 2A, B). The effect of Mn deficiency on wild type was variable between different experiments: wild-type rosette biomass was not reduced in the experiment displayed in Figure 2C and reduced by 45% compared to control conditions in the experiments shown in Figure 2D and Table I. By contrast, *nramp3nramp4* consistently displayed a much stronger growth reduction than wild type under Mn deficient conditions (63% in Figure 2C to 86% in Figure 2D, *n* = 4 independent biological replicates; Table I). Qualitatively similar results were obtained in hydroponic culture (Figure S3A). Under Mn deficiency, *nramp3nramp4* mutant leaves were not curled but their size was reduced in comparison with wild type (Figure 2B). The rosette biomass of *nramp3* and *nramp4* single mutants was indistinguishable from the wild type (Figure 2C), indicating that AtNRAMP3 and AtNRAMP4 are functionally redundant under Mn-deficient conditions. Measurements of dry biomass gave comparable results indicating that the water content was similar between wild-type, *nramp3*, *nramp4* and *nramp3nramp4* plants grown either under control conditions or under Mn deficiency (data not shown). The growth phenotype of the *nramp3nramp4* mutant under Mn deficiency could be rescued by introduction of *AtNRAMP3* or *AtNRAMP4* wild-type genes in the *nramp3nramp4* mutant background (Figure 2D and S2).

The growth defect of the *nramp3nramp4* mutant is not associated with reduced Mn concentrations in leaves or mesophyll protoplasts

To test whether the lower growth of *nramp3nramp4* mutants under Mn deficiency is associated with a decreased Mn content in leaves or mesophyll cells, metal concentrations in leaves and metal contents of mesophyll protoplasts were measured by ICP-AES in plants grown on perlite under controlled mineral nutrition. Plants were watered either with control Mn-sufficient nutrient solution (C) or with a nutrient solution lacking Mn (- Mn). Upon growth under control conditions, no differences in leaf metal concentrations were observed between wild-type and *nramp3nramp4* mutant plants for Fe, Mn and Zn (Figure 3A). In wild-type and *nramp3nramp4* mutant plants, growth under Mn deficient conditions resulted in a decrease in leaf Mn

9

concentrations by about 90% when compared to plants grown under control conditions; in wild-type plants grown under Mn-deficient conditions, Fe concentrations were unchanged and Zn concentrations were slightly increased (Figure 3A). Fe, Mn and Zn concentrations in leaves of the *nramp3nramp4* mutant grown under Mn-deficient conditions were significantly higher than in leaves of the wild type in the same conditions. No statistically significant differences were detected between either *nramp3* or *nramp4* single mutant and wild-type rosette metal concentrations for any of the three metals Fe, Mn or Zn (Table SI).

For Fe and Zn, relative metal concentrations in mesophyll protoplasts isolated from plants grown under control or Mn deficient conditions followed a similar pattern as leaf metal concentrations (Figure 3B, left and right panel). Mn concentrations in *nramp3nramp4* mutant protoplasts were 2 to 3-fold higher than in wild-type protoplasts under control (Mn- sufficient) conditions. This result is in agreement with the result obtained on mesophyll protoplasts from plants grown on soil (Figure 1B). In contrast, under Mn deficiency, relative Mn concentrations in wild-type and *nramp3nramp4* mutant protoplasts were not statistically different (Figure 3B).

Taken together, these data demonstrate that Mn concentrations in *nramp3nramp4* leaves or mesophyll protoplasts, respectively, are equal or higher than in the wild type, under both control and Mn deficient conditions. This result excludes that a defective Mn supply to *nramp3nramp4* mesophyll cells is responsible for the growth defect of this mutant under Mn deficiency.

The level of active Photosystem II is lower in *nramp3nramp4* mutant under Mn deficiency

Manganese is an essential cofactor of the water splitting complex of photosystem II (PS II). Therefore, the growth defect observed in *nramp3nramp4* under Mn-deficient conditions could be explained by a defect in the ability to split water, leading to a lower activity of photosynthesis. Since a defect in PS II can be detected through the quantification of chlorophyll fluorescence, the ratios Fv/Fm were measured in wild-type and *nramp3nramp4* plants (Maxwell and Johnson, 2000).

Ratios Fv/Fm close to 0.8 obtained for wild-type, *nramp3*, *nramp4* and *nramp3nramp4* plants grown under control (Mn sufficient) conditions are consistent with ratios reported for *Arabidopsis thaliana* and other higher plants (Björkman and Demmig, 1987)(Table I and SII, Figure S4). In Mn deficient plants, the ratio dropped to 0.65 for wild-type plants and was further significantly reduced to 0.57 in the

nramp3nramp4 plants (Table I). This indicates a decline of the photosynthetic efficiency under Mn deficiency, which is exacerbated in the nramp3nramp4 mutant compared to the wild type. Fv/Fm ratios were rescued to values equal or higher than wild type in nramp3nramp4 mutant lines complemented by AtNRAMP3 or AtNRAMP4 (Table SII). In the same conditions, Fv/Fm ratios in nramp3 and nramp4 single mutants, respectively, were not significantly lower than in the wild type, confirming the functional redundancy of these two genes (Figure S4). Upon prolonged growth in Mn deficient conditions for an additional 3 weeks, Fv/Fm ratio dropped to similarly low values for wild type, nramp3, nramp4 and nramp3nramp4 (Figure S4).

To further investigate the effect of Mn deficiency on PSII, thermoluminescence measurements were performed on intact leaves of plants grown under Mn deficient and sufficient conditions on perlite for 8 weeks. In thermoluminescence measurements, the emitted light originates from charge recombinations of trapped charge pairs within PS II (Inoue, 1996). The charge pairs involved can be identified by their emission temperature, which strongly depends on the redox potentials of the charge pairs. The most important thermoluminescence band for investigating the electron transfer within PSII is the B-band. Recombination of S_2 or S_3 state of the oxygen-evolving complex at the donor side of PSII with the semi-reduced secondary quinone acceptor in PSII, Q_B^-, yields the B-band at around 30°C (Rutherford et al., 1982). Figure 4A shows the changes in the intensity of the B-band at 24°C recorded from leaves of dark-adapted plants in dependence on the number of exciting single turnover flashes. As expected for leaves, the highest intensity of the B-band was observed after the second flash and the intensity of this band oscillates with a period of 4. This oscillation reflects the cycle of the oxidation states of the Mn cluster (S_{0-4}) (Figure 4A). In nramp3nramp4 leaves, the intensity of the B-band was strongly reduced. A normal oscillation pattern was still observed during the first four flashes. This was dampened almost completely when more flashes were given (Figure 4A). These results show that the function of the water-splitting complex is normal in nramp3nramp4, but that only very few Mn clusters are functional in the nramp3nramp4 double mutant. A low intensity of the flash-induced B-band has been described previously in tobacco plants in which the level of PsbP was severely down-regulated by the RNA interference technique. In these plants the Mn cluster of PSII is very unstable and disassembles quickly in the dark (Ifuku et al., 2005).

1   In Mn deficient *nramp3nramp4* plants, PS II was highly susceptible to

2   illumination with high light (Figure 4B). When leaves of Mn-deficient *nramp3nramp4*

3   plants were exposed to high light intensities (2000 μmol quanta m^{-2} s^{-1}) for 1 h, the

4   variable fluorescence was lowered to values below the fluorescence level measured

5   with the low intensity measuring light on dark adapted leaves (Figure 4B, upper left

6   panel). This indicates that the plastoquinone pool was partially reduced in the dark-

7   adapted plants prior to the measurements (Bondarava et al., 2003). During a

8   subsequent period of incubation in dim light for 3 h, the variable fluorescence probed

9   by short flashes of actinic light did not recover, suggesting that the repair of

10   photoinhibited PS II was not achieved. In the presence of Mn, the mutant showed a

11   much lower loss of variable fluorescence (lower left panel), and the recovery of the

12   variable fluorescence was similar to that of wild type grown under identical conditions

13   (lower right panel).

14

15   The level of D1 (PsbA), the core protein of PS II which binds the Mn cluster,

16   was analyzed by immunoblotting in wild-type and *nramp3nramp4* leaves from plants

17   grown under control and Mn deficient conditions. In plants grown under Mn sufficient

18   conditions D1 protein levels were higher in *nramp3nramp4* than in wild-type leaves

19   (Figure 4C and S5). The amount of D1 was strongly reduced in Mn deficient wild-type

20   leaves, and even further reduced in Mn-deficient *nramp3nramp4* mutant plants

21   (Figure 4C and S5). The decreased abundance of D1 protein in Mn deficient

22   *nramp3nramp4* mutant leaves is in agreement with the observation of a lower

23   number of active PS II in these plants (Table 1, Figure S4).

24   The growth defect observed in the mutant under Mn deficiency is thus

25   associated with a severe decrease in the number of functional PS II centers. To test

26   whether the decrease in the number of functional PS II is associated with a shortage

27   of Mn, we measured the relative Mn concentrations in chloroplasts isolated from

28   mesophyll cells of wild-type and *nramp3nramp4* plants grown under control and Mn

29   deficient conditions. Relative Mn concentrations were similar in chloroplasts from wild

30   type and *nramp3nramp4* grown under control conditions. The Mn concentrations in

31   chloroplasts of Mn-deficient wild-type plants was reduced to 50% of that of control

32   plants (Figure 4D). Under Mn deficiency, *nramp3nramp4* mutant chloroplasts

33   exhibited merely about half of the Mn concentration found in wild type. This result

34   suggests that a reduced availability of Mn to form Mn clusters in the chloroplasts is a

1 cause of the lower number of active PS II in the mutant under Mn deficiency. Taken

2 together, these data indicate that under Mn deficiency, the defect in Mn export from

3 the vacuole in *nramp3nramp4* perturbs Mn allocation to the chloroplast and leads to

4 a lower number of active PS II.

5 **Manganese dependent Superoxide Dismutase activity is not reduced in**

6 *nramp3nramp4* **mesophyll cells**

7 As the defect in Mn export from the vacuoles of *nramp3nramp4* reduces the number

8 of functional PS II in leaves under Mn deficiency, we tested whether the function of

9 the other quantitatively major Mn-dependent protein, MnSOD, is defective in this

10 mutant. In-gel measurements of SOD activity were performed after separation by

11 native PAGE of total protein extracts from leaves of wild type and *nramp3nramp4*

12 mutants grown on perlite under control conditions, Fe deficiency or Mn deficiency.

13 Three bands were detected that displayed SOD activity (Figure 5A). On the basis of

14 inhibition by KCN (not shown) and H_2O_2 (Figure 5B), the bands could be assigned to

15 CuZnSOD (KCN and H_2O_2 sensitive), FeSOD (H_2O_2 sensitive) and MnSOD

16 (insensitive to KCN and H_2O_2). Under Fe deficiency, FeSOD activity was strongly

17 reduced in both wild-type and *nramp3nramp4* mutant leaves (Figure 5A). Under Mn

18 deficiency, MnSOD was neither strongly decreased in the wild type nor in the

19 *nramp3nramp4* double mutant (Figure 5B). These data show that in contrast to PS II

20 function, MnSOD activity, which is known to be localized in the mitochondria, is

21 maintained in the *nramp3nramp4* mutant under Mn deficiency.

22 **Regulation of AtNRAMP3 and AtNRAMP4 protein levels**

23 Previous results indicated that in seedlings, AtNRAMP3 and AtNRAMP4 expression

24 levels are regulated in response to Fe status (Thomine et al., 2003; Lanquar et al.,

25 2004; Lanquar et al., 2005). The results obtained in the present study suggested an

26 important role of AtNRAMP3 and AtNRAMP4 in Mn distribution to PS II under Mn

27 deficiency. Therefore, the regulation of AtNRAMP3 and AtNRAMP4 protein levels

28 was reexamined in adult plants grown under Fe or Mn deficient conditions. Wild-type

29 and *nramp3nramp4* plants were grown hydroponically under control (C), Fe deficient

30 (- Fe) and Mn deficient (- Mn) conditions. In Fe-deficient plants, Fe concentrations

31 were decreased by 85% in shoots and 90% in roots of both genotypes when

32 compared to controls (Figure S3B) while Mn accumulation was increased as

33 previously described (Vert et al., 2002). In Mn-deficient plants, Mn concentrations

34 were decreased by 90% in shoots and 80% in roots when compared to controls

13

(Figure S3B). Concentrations of other cations were unchanged. AtNRAMP3 and AtNRAMP4 protein levels were analyzed by immunoblot in 3 biological replicates. Under Fe deficiency, AtNRAMP3 protein levels increased in roots (in 2 out of 3 experiments) but did not show any regulation in shoots of adult plants (Figure 6A). Levels of AtNRAMP4 protein increased under iron deficiency in both shoots (in 3 out of 3 experiments) and roots (in 2 out of 3 experiments). These results are consistent with previous reports (Thomine et al., 2000; Lanquar et al., 2005). In contrast, these experiments did not reveal any significant regulation of AtNRAMP3 or AtNRAMP4 protein levels in response to Mn deficiency (Figure 6A). In addition, staining of promoter AtNRAMP3::GUS (Thomine et al., 2003) or promoter AtNRAMP4::GUS (Lanquar et al., 2005) seedlings grown for 7 days on agar based medium containing either no Mn (- Mn) or 0.1 mM Mn (control) did not exhibit any Mn-dependent regulation of *AtNRAMP3* or *AtNRAMP4* promoter activity (data not shown and Lanquar et al. 2005).

Ferritin protein levels are up-regulated in *nramp3nramp4* mutants under Mn deficiency

The specific up-regulation of AtNRAMP3 and AtNRAMP4 under Fe deficiency, although they are primarily involved in Mn mobilization from the vacuole in adult plants, is intriguing. To further investigate this apparent link between Fe and Mn homeostasis, the level of ferritin 1 protein, AtFER1, was monitored in leaves of wild-type and *nramp3nramp4* plants grown hydroponically under control, Mn-deficient (- Mn) and Fe-deficient (- Fe) conditions. Immunoblots to detect AtFER1 were performed on four independent biological replicates. Ferritins store Fe in non-toxic form in the stroma of chloroplasts (Briat et al., 1999). In plants grown under control conditions, the levels of AtFER1 in shoots were unchanged in the double mutant (in 3 out of 4 experiments) (Figure 6B). Under Fe deficiency, AtFER1 is neither detectable in the wild type nor in the double mutant (in all 4 experiments), as described previously (Ravet et al., 2009a). Under Mn deficiency, the amount of AtFER1 in wild-type plants was slightly decreased compared to the signal observed in control conditions (in 2 out of 4 experiments), or unchanged (in 2 out of 4 experiments). Interestingly, in Mn-deficient *nramp3nramp4* plants, the amount of ferritin 1 was consistently between 3.5 and 7 times higher when compared to wild type grown under the same conditions (in 4 out of 4 experiments; Figure 6B). This increase was consistently observed in plants grown in perlite watered with – Mn medium, in plants

14

1   grown hydroponically in - Mn medium and in two week-old-plants grown on Mn-

2   deficient agar medium. The up-regulation of AtFER1, a component of Fe

3   homeostasis in the shoots of *nramp3nramp4* mutants under Mn deficiency suggests

4   a higher iron status in chloroplasts of *nramp3nramp4* mutants compared to wild type

5   under these conditions. This is in agreement with the higher iron concentrations in

6   leaves and protoplasts from Mn deficient *nramp3nramp4* compared to wild type

7   (Figure 3).

8   To test whether other components of the Fe homeostasis network were also

9   deregulated, the levels of AtFER1 and AtIRT1 were monitored in the roots. Protein

10   extracts from 2 biologically independent replicates were analyzed. AtIRT1 is the high

11   affinity Fe transporter, and IRT1 protein levels are up-regulated under Fe deficiency

12   (Connolly et al., 2002; Seguela et al., 2008). IRT1 was detected only in roots of Fe-

13   deficient plants and protein levels were equivalent in wild-type and *nramp3nramp4*

14   plants (Figure 6B). This is different from the finding in barley, where HvIRT1 is up-

15   regulated in response to both Fe and Mn deficiency (Pedas et al., 2008). AtFER1

16   protein levels were equivalent in roots of wild-type and *nramp3nramp4* plants under

17   control and Mn deficient conditions (data not shown).

18

19   **Discussion**

20   The results presented in this study demonstrate that AtNRAMP3 and AtNRAMP4 are

21   involved in Mn homeostasis in the adult plant. The strong accumulation of Mn in

22   *nramp3nramp4* mutant mesophyll vacuoles suggests that in this tissue, AtNRAMP3

23   and AtNRAMP4 participate in the release of Mn from the vacuoles (Figure 1). Under

24   Mn deficiency, *nramp3nramp4* double mutant plant growth is reduced (Figure 2). This

25   growth defect correlates with a lower number of functional PS II, consistent with a

26   shortage of Mn to form Mn clusters (Figure 3).

27   **AtNRAMP3 and AtNRAMP4 operate in the retrieval of Mn from vacuoles in leaf**

28   **mesophyll cells**

29   Mesophyll vacuoles of adult *nramp3nramp4* plants contain substantially higher

30   amounts of Mn than those of the wild type (Figure 2). This result suggests a function

31   of AtNRAMP3 and AtNRAMP4 in the retrieval of Mn from vacuoles. Transfer of Mn

32   into and retrieval from vacuoles thus appears to proceed continuously in the wild

33   type, resulting in the accumulation of, on average, only 10% of protoplast Mn inside

34   vacuoles in the steady state (Figure 1B). The results obtained here suggest that the

1 mesophyll vacuole is predominantly a compartment for Mn transit rather than for Mn

2 storage. Despite the strongly enhanced accumulation of Mn in vacuoles of the

3 *nramp3nramp4* mutant, global leaf Mn concentrations are barely increased when

4 compared to the wild type (Figure 1, 3, S3). This could be due to the fact that the

5 mesophyll intracellular Mn pool accounts for only a minor part of total leaf Mn. Mn

6 concentrated in the cell wall or in other leaf cell types, such as vascular bundles or

7 epidermal cells, could mask differences between the mesophyll cells of different

8 genotypes. Alternatively, in the mutant, the increase in mesophyll vacuolar Mn

9 contents could be compensated by a reduction in Mn contents in a different cell type.

10 Lack of AtNRAMP3 and AtNRAMP4 leads to a modification of the subcellular

11 distribution of Mn. While mesophyll vacuoles of wild-type plants grown on soil contain

12 on average 10% of total Mn pool in mesophyll protoplasts, vacuoles isolated from the

13 mutant contain on average 70% of the intracellular Mn. By contrast, 92% and 80% of

14 the total protoplast Zn pool was associated with the vacuoles of wild-type and mutant

15 mesophyll cells, respectively. The finding that only 10% of the Mn is associated with

16 wild-type vacuoles is surprising in view of other studies indicating that most Mn is

17 stored in the vacuole. Based on Mn broadening of ^{31}P NMR signal or on the analysis

18 of ^{54}Mn radiotracer release kinetics, Quiquampoix et al. and Pedas et al. concluded

19 that most Mn is stored in the vacuoles of maize and barley root cells, respectively

20 (Quiquampoix et al., 1993; Pedas et al., 2005). The discrepancy with our results may

21 be explained by the use of different experimental approaches or by a different

22 intracellular distribution of Mn in root and mesophyll cells or by differences in Mn

23 storage between species. González and Lynch reported that most Mn is stored in the

24 vacuole of bean leaf cells (González and Lynch, 1999). However, their study

25 addressed Mn storage under Mn excess, a condition in which vacuolar Mn

26 sequestration may be favored.

27 Iron was also detected in mesophyll vacuoles of wild-type and double mutant plants.

28 Although AtNRAMP3 and AtNRAMP4 are capable of Fe transport (Thomine et al.,

29 2000; Lanquar et al., 2005), no difference between the Fe content of *nramp3nramp4*

30 and wild-type vacuoles was detected (Figure 1), even when vacuoles were isolated

31 from the mesophyll of Fe deficient plants (data not shown). Thus, AtNRAMP3 and

32 AtNRAMP4 are not likely to be required for Fe export from the vacuole in this tissue.

33 However, the relatively high variation between biological replicates could mask small

1   differences in Fe contents between wild-type and the *nramp3nramp4* double mutant

2   vacuoles.

3   **Under Mn deficiency, optimal Mn supply to chloroplasts requires**

4   **AtNRAMP3/AtNRAMP4-dependent Mn transit through the vacuole**

5   When plants are grown in control conditions, the high amount of Mn retained in

6   *nramp3nramp4* vacuoles does not lead to any reduction in plant growth (Figure 2,

7   S3). This suggests that, although a large proportion of cellular Mn transits through

8   the vacuole in the mesophyll of wild-type plants, a lack of AtNRAMP3/AtNRAMP4-

9   dependent Mn retrieval from the vacuole does not limit cellular Mn supply. However,

10 under Mn deficiency, *nramp3nramp4* plants display a strong growth reduction (Figure

11 2). This growth inhibition is not associated with a lower Mn pool in mesophyll cells

12 (Figure 3), but with an alteration of the intracellular distribution of Mn instead.

13 Chloroplast Mn concentrations of Mn deficient *nramp3nramp4* plants were much

14 lower than in wild-type plants (Figure 4). The intracellular Mn that is missing in the

15 chloroplasts of *nramp3nramp4* plants is likely sequestered in the vacuoles, based on

16 the results obtained using Mn sufficient plants (Figure 2). These results suggest that,

17 under Mn deficiency, transit of Mn through the vacuole becomes a limiting pathway

18 for the distribution of this metal to indispensable Mn-requiring proteins. Mn is an

19 important cofactor of the oxygen-evolving complex of PS II. Compared to the wild

20 type, a lower number of functional PS II correlated with an enhanced impact of Mn

21 deficiency on biomass production in the double mutant. By contrast, mitochondrial

22 MnSOD activity was not decreased under Mn deficiency in the wild type or in

23 *nramp3nramp4*. The results presented suggest that under Mn deficiency, the use of

24 the vacuolar Mn pool is required for optimal photosynthesis and plant growth but not

25 for providing Mn cofactor to MnSOD in mitochondria. In contrast, in *C. reinhardtii*, Mn

26 deficiency leads to a decrease in both PS II fluorescence and MnSOD activity (Allen

27 et al., 2007). In Arabidopsis mesophyll cells, the oxygen evolving complex of PS II

28 thus appears as a major Mn requiring enzyme, and its activity is more sensitive to Mn

29 deficiency than that of MnSOD, in agreement with previous work on other plants

30 (Marschner, 1995). In yeast, SMF2, a membrane protein of the NRAMP family

31 localized in intracellular vesicles, plays a role in providing Mn to mitochondrial SOD

32 (Luk and Culotta, 2001). In Arabidopsis, this role could be played by another Mn

33 transport pathway distinct from AtNRAMP3 and AtNRAMP4. The results presented

34 here underline the importance of Mn transit through the vacuole for Mn supply to the

17

1 chloroplast under conditions of Mn deficiency, whereas under Mn sufficient
2 conditions Mn transit through the vacuole is not required to maintain the primary Mn-
3 dependent chloroplast function. Under Mn deficiency, the cellular Mn uptake is
4 strongly reduced due to low external availability, and we hypothesized that cellular
5 Mn recycling following protein degradation becomes substantially more important.
6 Cellular Mn recycling is likely to involve passage through the vacuole as a
7 compartment known to be involved in organelle autophagy (Wada et al., 2009). We
8 speculate that under Mn deficiency and non-excess Mn sufficiency, Mn transit
9 through the vacuole is part of a continuous cellular recycling pathway for Mn
10 involving AtNRAMP3 and AtNRAMP4, which becomes essential for the maintenance
11 of photosynthesis and growth under conditions of Mn deficiency. However, as the
12 results presented in Figure 1A do not formally exclude that AtNRAMP3 and
13 AtNRAMP4 may reside on other membranes than the tonoplast, the possibility
14 remains that *nramp3nramp4* phenotype is also related to a defect in Mn transport to
15 or from another intracellular compartment.

16 **AtNRAMP3 and AtNRAMP4 have redundant functions in mesophyll cells**
17 Under Mn deficiency, decreases in plant biomass production and maximum quantum
18 yield were only observed in the *nramp3nramp4* double mutant, and not in *nramp3*
19 and *nramp4* single mutants (Figure 2, S4). This result indicates that *AtNRAMP3* and
20 *AtNRAMP4* genes have redundant functions in Mn homeostasis in leaves. This is in
21 agreement with previous reports on the redundant function of AtNRAMP3 and
22 AtNRAMP4 in Fe mobilization during seed germination and in cadmium tolerance
23 (Lanquar et al., 2005; Oomen et al., 2009). By contrast, AtNRAMP3 and AtNRAMP4
24 functions in pathogen resistance are additive (Segond et al., 2009). Overlapping, but
25 not fully identical localization of *AtNRAMP3* and *AtNRAMP4* promoter activity
26 (Thomine et al., 2003; Lanquar et al., 2005), and circumstantial evidence for a higher
27 abundance of the AtNRAMP4 protein in mesophyll cells when compared to
28 AtNRAMP3 (Carter et al., 2004) support both the possibility of functional redundancy
29 as well as of functional differentiation between the two proteins.

30 **Cross talk between Fe and Mn homeostasis**
31 Although other NRAMP family members in yeast, *C. reinhardtii* and bacteria are up-
32 regulated under Mn deficiency, neither AtNRAMP3 nor AtNRAMP4 is regulated in
33 response to Mn deficiency at the protein level (Portnoy et al., 2000; Patzer and
34 Hantke, 2001; Allen et al., 2007). It is possible that the expression level of

18

1   AtNRAMP3 and AtNRAMP4 observed under control conditions is sufficient to support

2   sufficient rates of Mn retrieval from vacuoles also under Mn deficiency. Alternatively,

3   the transport activity of these proteins might be regulated at a different level. In

4   contrast, AtNRAMP3 and AtNRAMP4 protein abundance is up-regulated in response

5   to Fe deficiency (Figure 6) (Lanquar et al., 2005). This suggests that AtNRAMP3 and

6   AtNRAMP4 may play a role during iron deficiency in adult plants, which remains to

7   be identified. Previous report showed that, in *nramp3* knockout mutants, Mn

8   accumulation is increased under severe Fe deficiency (Thomine et al., 2003).

9   Conversely, Mn accumulation under Fe deficiency is reduced in 35S-*AtNRAMP3*

10 Arabidopsis lines (Thomine et al., 2003). This effect was associated with similar

11 changes in Zn accumulation and other responses to Fe deficiency, suggesting that

12 AtNRAMP3 modulates responses to Fe deficiency (Baxter et al., 2008). In the

13 present study, no difference in Mn accumulation was detected between adult wild-

14 type and *nramp3nramp4* plants grown under Fe deficiency (Figure S3). In *C.*

15 *reinhardtii*, Mn deficiency leads to secondary iron deficiency (Allen et al., 2007).

16 Under the conditions used in this study, none of the Arabidopsis Fe deficiency-

17 responsive proteins analyzed, AtNRAMP3, AtNRAMP4 or IRT1, is up-regulated

18 under Mn deficiency indicating that Mn deficiency does not trigger secondary Fe

19 deficiency.

20 Increased accumulation of ferritin 1 and an increase in iron concentration in leaves of

21 *nramp3nramp4* plants grown under Mn deficiency suggests a coordinated

22 homeostasis of Mn and Fe (Figures 3, 6). It was shown that, in *C. reinhardtii*, Fer1 is

23 up-regulated under iron deficiency. It has been proposed that CrFer1 functions to

24 buffer the iron released as a consequence of the degradation of some Fe-containing

25 proteins of the photosynthetic apparatus (Long et al., 2008). In Arabidopsis, ferritins

26 have recently been shown to be necessary to prevent oxidative damage originating

27 from the presence of free Fe in plastids when plants are exposed to excess Fe

28 (Ravet et al., 2009a). In microorganisms, Mn plays a role in protection against

29 oxidative stress (Anjem et al., 2009). During Mn deficiency, increased degradation of

30 photosynthetic proteins leading to the release of free Fe or decreased Mn protective

31 effect could lead to oxidative stress. The observed increase in ferritin levels could

32 buffer iron and prevent oxidative damage.

33

34

19

Materials and methods

Plant material

The generation of the *nramp3-1* single mutant, the 35S-*AtNRAMP3* lines, the *nramp3nramp4* double mutant and the complemented lines *nramp3nramp4* AtNRAMP3 and *nramp3nramp4* AtNRAMP4 were described previously (Thomine et al., 2003; Lanquar et al., 2005).

Growth conditions

For perlite growth experiments, perlite (Puteaux fournitures horticoles, Les Clayes-sous-Bois, France) was washed once with 2.5 mM EGTA and then with about 10 volumes of deionized water. Arabidopsis seeds were sown on perlite and watered with a modified Hoagland's solution (0.28 mM KH_2PO_4, 1.25 mM KNO_3, 0.75 mM $MgSO_4$, 1.5 mM Ca(NO3)$_2$, 25 µM H_3BO_3, 50 µM KCl, 1 µM $ZnSO_4$, 0.1 µM Na_2MoO_4, 0.5 µM $CuSO_4$, 10 µM FeHBED, 3 mM MES-KOH, pH 5.7). Iron was provided as Fe^{3+} chelated to HBED (N,N'-di(2-hydroxybenzyl) ethylene diamine-N,N'-diacetic acid monochloride hydrate; Strem chemicals, Newburyport MA, USA). FeHBED was prepared as described (Lanquar et al., 2005). Plants were grown for 6 to 9.5 weeks with (C) or without 5 µM $MnSO_4$ (- Mn).

For the hydroponic growth experiments, seeds were surface sterilized and sown on bottom-cut 0.5 mL Eppendorf tubes filled with 0.8 % (w/v) Noble agar. For the first week, 6 seeds were placed in 500 mL of 0.5X Hoagland medium supplemented with 20 µM FeHBED and with (C and - Fe) or without 5 µM $MnSO_4$ (- Mn). Then, plants were grown either for 5 more weeks in 1X Hoagland medium supplemented with 10 µM FeHBED and with (C) or without 5 µM $MnSO_4$ (- Mn) or for 3 weeks in medium supplemented with 10 µM FeHBED, 5 µM $MnSO_4$ and then transferred into a medium supplemented with 5 µM $MnSO_4$ and 20 µM Ferrozine (- Fe) for 2 weeks. For culture on soil, on perlite or in hydroponics, plants were grown in a climate chamber, under the following conditions: 9/15h light/dark; light intensity 200 µE m^{-2} s^{-1}; constant temperature of 21°C; 60% rel. humidity).

Vacuole isolation

After removing the abaxial epidermis by rubbing on P600 sandpaper Arabidopsis leaves of plants grown on soil for 6 weeks, protoplasts were isolated by enzymatic

20

1 digestion of ~2 g of leaves in 50 mL MCP [500 mM Sorbitol, 1 mM $CaCl_2$, 10 mM

2 MES, pH 5.6 (KOH)] supplemented with 0.03% (w/v) Pectolyase Y23 (Yakult

3 Pharmaceuticals Ind.) and 0.75 % (w/v) Cellulase R10 (Yakult Pharmaceuticals Ind.)

4 at 23°C for 2 h. Protoplasts were filtered through a 75-μm nylon mesh, pelleted

5 (100g, 5 min) and washed twice with MCP; *ca.* 2 x10^8 protoplasts were obtained.

6 Protoplasts were diluted to 15-20 x 10^6 cells mL^{-1}, and were lysed by addition of an

7 equal volume of protoplast lysis buffer [200 mM Sorbitol, 10 % (w/v) Ficoll 400, 20

8 mM EDTA, 10 mM HEPES pH 8 (KOH), 0.15 % (w/v) BSA, 2 mM dithiothreitol (DTT)]

9 prewarmed to 42°C. Protoplast lysis was monitored microscopically, and lysed

10 protoplasts were kept on ice. Vacuoles were isolated and concentrated using a step

11 gradient prepared on ice (1500 g, 20 min, 4°C): bottom phase, 1 volume of lysed

12 protoplasts; middle phase, 0.8 volume of lysis buffer diluted in vacuole buffer to reach

13 a concentration of 4 % (w/v) Ficoll; top phase, 0.2 volume of vacuole buffer [500 mM

14 Sorbitol**,** 10 mM HEPES, pH 7.5 (KOH)**,** 0.15 % (w/v) BSA, 1 mM DTT, 2 μg mL^{-1}

15 leupeptine, 2 μg mL^{-1} antipaine]. Vacuoles were recovered at the interface between

16 the middle phase and the top phase. Purity of the vacuole preparation was monitored

17 by microscopy; *ca.* 2 x 10^7 vacuoles were obtained in total.

18 For immunoblot analysis, after isolation, vacuoles were lysed as follows: 1 volume of

19 vacuoles was mixed by inversion with 3 volumes of 50 mM MOPS pH 7.8, 0.1 mM

20 DTT and 1X Complete Protease Inhibitor Cocktail Tablets (Roche Applied Science).

21 The vacuolar membrane was collected by ultracentrifugation at 110,000 g at 4°C for

22 90 min, and the pellet was resuspended in the same MOPS-DTT buffer. Protein

23 concentration was determined by the Bradford method.

24

25 **Chloroplast isolation**

26 Protoplasts were isolated and lysed as described above for the isolation of vacuoles.

27 Percoll gradients were prepared by ultracentrifugation (40'000 g, 55 min, 4°C, without

28 brake): bottom phase, 1 volume 100% Percoll; top phase: 1 volume of washing

29 medium [300 mM Sorbitol, 40 mM TRICINE pH 7.6, 2.5 mM EDTA, 0.5 mM $MgCl_2$]

30 and kept at 4°C. Chloroplasts were isolated by loading 6 ml of protoplast lysate on

31 the preformed Percoll gradient followed by centrifugation (13'000 g, 10 min, 4°C,

32 without brake). Intact chloroplasts were recovered at the bottom of the tube and were

33 washed four times with cold washing medium (Ferro et al., 2002). Purity and integrity

1 of the chloroplast preparation was monitored by microscopy and the amount of
2 chloroplasts was evaluated by measurement of the chlorophyll content.
3
4 **Protein isolation**
5 Total protein extracts from protoplasts, shoots and roots were prepared by
6 homogenization in 50 mM HEPES NaOH pH 7.2, 1.5 mM $MgCl_2$, 1 mM EGTA, 1 mM
7 EDTA, 10 % (w/v) Glycerol, 1 % (v/v) Triton-X100, 150 mM NaCl, 5 mM DTT and 1X
8 Complete Protease Inhibitor Cocktail Tablets (Roche Applied Science). Samples
9 were then centrifuged for 10 min, 1000 g at 4°C and supernatants were recovered.
10 Protein concentration was estimated by the Bradford method.
11
12 **Immunoblot analysis**
13 Unless specified, 15 μg of vacuolar membrane, protoplast, root or shoot proteins
14 were separated on SDS-PAGE and immunoblot analysis was performed. Rabbit anti-
15 AtNRAMP3 polyclonal antibodies were raised against two synthetic peptides
16 corresponding to N-terminal and C-terminal regions of AtNRAMP3 protein (N-term
17 H2N-MPQLENNEP LLINEC-CONH2 ; C-term H2N-CTPWPFKAESSH–COOH)
18 (Eurogentec). The anti-AtNRAMP3 antibodies were affinity-purified against the same
19 peptides.
20 The antibodies used in this study were diluted as follows: AtNRAMP3 1:1000;
21 AtNRAMP4 1:2000, AtVPPAse 1:20.000 dilution (Sarafian et al., 1992), AtFerritin
22 1:10.000 (Dellagi et al., 2005), AtIRT1 1/8000 (Seguela et al., 2008) PsbA/D1
23 1/15.000 (Agrisera, Sweden). Immunoblots were performed as described previously
24 (Lanquar et al., 2005).
25
26 **Metal content measurements**
27 Leaves, shoots and roots were harvested separately and washed. Roots were
28 desorbed by incubation in ice cold buffer containing 5 mM $CaCl_2$, 1 mM MES KOH
29 pH 5.7 for 10 min. The dry biomass (DW) of the samples was measured after drying
30 at 60°C. Protoplast and vacuole samples were concentrated in a SpeedVac® after
31 determination of the number of vacuoles or protoplasts per sample by counting
32 objects under the microscope. All samples were digested in 65% nitric acid in a
33 MARS5 microwave (CEM GmbH, Kamp-Lintford, Germany) at 200°C at 15 bar for 10
34 min. After dilution in trace metal free water, the metal content of the samples was

1 determined by inductively coupled plasma atomic emission spectroscopy (ICP-AES)

2 using an IRIS Advantage Duo ER/S (Thermo Jarrell Ash, Franklin, MA, USA) as

3 described (Lanquar et al., 2005). The metal concentrations were expressed either as

4 mg kg^{-1} DW for tissue samples, pg per object for protoplasts and vacuoles, or relative

5 to the geometric mean of a combination of elements: Ca, Cu, Fe, Mg, Mn, Mo, P and

6 Zn for protoplasts; Cu, P and S for chloroplasts. Note that other elements could not

7 be used because of contaminant levels in the buffer in which chloroplasts were

8 suspended.

9

10 **Chlorophyll fluorescence measurements.**

11 Room temperature chlorophyll fluorescence was measured *in vivo* using a pulse-

12 amplitude modulation fluorimeter (PAM 101-3, Walz, Effeltrich). The intensity of the

13 measuring light (standard PAM 101set) was sufficiently low (integral intensity about

14 10^{-8} mol quanta m^{-2} s^{-1}, frequency of modulated light: 1.6 kHz) to prevent the

15 reduction of plastoquinone. Saturating flashes (1 s) were given to measure the

16 maximum fluorescence. Efficiency of the photochemical electron transport was

17 assayed by calculating the ratio of variable fluorescence Fv to maximal fluorescence

18 Fm (Fv/Fm) (Maxwell and Johnson, 2000). In all experiments, the Fv/Fm ratio was

19 measured on leaves of dark adapted plants. As photoinhibitory white light (Figure

20 4B), a cold light source was used with an intensity of 2000 μmol quanta m^{-2} s^{-1}.

21 Recovery was followed for 3 h in dim white light (5 μmol quanta m^{-2} s^{-1}).

22

23 **Thermoluminescence measurements**

24 Thermoluminescence was measured with a home-built apparatus. To measure the

25 thermoluminescence originating from the $S_{2/3}Q_B^-$ charge recombination (B band),

26 excised leaf pieces were incubated in the dark at 20°C for 5 min and then flashed

27 with saturation Xenon flashes at 1°C (1 s interval between flashes). Samples were

28 heated with a constant rate (0.4°C s^{-1}) from 1°C to 70°C and the light emission was

29 recorded. Graphical and numerical data analyses were performed as described

30 (Ducruet and Miranda, 1992).

31

32 **Superoxide dismutase activity**

33 Total leaf protein extracts were prepared by homogenization in 100 mM potassium

34 phosphate pH 7, 3.5 mM DTT, 1 mM EDTA, 1 mM PMSF, 15% (v/v) glycerol, 1%

23

1 (w/v) PVP (polyvinylpyrrolidone), 0.1% (v/v) Triton X-100. Samples were centrifuged

2 (10'000 g, 5 min, 4°C) and supernatants were recovered. Protein concentration was

3 estimated by the Bradford method. Total protein extracts were separated on a native

4 polyacrylamide gel (12%, Precast Gel, BioRad, USA) and SOD activity was detected

5 in gel as described (Beauchamp and Fridovitch, 1971). FeSOD and CuZnSOD

6 activities were identified by sensitivity to 2 mM KCN for CuZnSOD and sensitivity to

7 5 mM H_2O_2 for CuZnSOD and FeSOD. Treatments were performed prior to activity

8 staining.

9

10 **Supplemental material**

11 Supplemental figure 1: characterization of an anti-AtNRAMP3 polyclonal antibody.

12 Supplemental figure 2: rescue of the *nramp3nramp4* growth defect in the absence of

13 manganese by *AtNRAMP3* or *AtNRAMP4*.

14 Supplemental figure 3: phenotype and metal content of *nramp3nramp4* plants grown

15 in hydroponic culture.

16 Supplemental figure 4: time course variations of Fv/Fm in wild type, *nramp3*, *nramp4*

17 and *nramp3nramp4* under Mn sufficient or deficient conditions.

18 Supplemental figure 5: quantification of D1 immunoblot and silver staining as loading

19 control.

20 Supplemental table 1: metal concentrations of wild-type and *nramp* mutant rosettes,

21 grown in presence (control) or absence of manganese (- Mn)

22 Supplemental table 2: chlorophyll fluorescence of complemented *nramp3nramp4*

23 plants.

24

25 **Acknowledgements**

26 The authors thank Drs F. Gaymard and C. Curie for sharing FER1 and IRT1

27 antibodies before publication.

28

29 **Literature cited**

30 **Allen MD, Kropat J, Tottey S, Del Campo JA, Merchant SS** (2007) Manganese
31 deficiency in Chlamydomonas results in loss of photosystem II and MnSOD
32 function, sensitivity to peroxides, and secondary phosphorus and iron
33 deficiency. Plant Physiol **143:** 263-277
34 **Anjem A, Varghese S, Imlay JA** (2009) Manganese import is a key element of the
35 OxyR response to hydrogen peroxide in *Escherichia coli*. Mol Microbiol **72:**
36 844-858

24

Baxter IR, Vitek O, Lahner B, Muthukumar B, Borghi M, Morrissey J, Guerinot ML, Salt DE (2008) The leaf ionome as a multivariable system to detect a plant's physiological status. Proc Natl Acad Sci U S A **105:** 12081-12086

Beauchamp C, Fridovitch I (1971) Superoxide dismutase: improved assays and an assay applicable to acrylamide gels. Anal. Biochem. **44:** 276-287

Björkman O, Demmig B (1987) Photon yield of O_2 evolution and chlorophyll fluorescence characteristics at 77 K among vascular plants of diverse origins Planta **170:** 489-504

Bondarava N, De Pascalis L, Al-Babili S, Goussias C, Golecki JR, Beyer P, Bock R, Krieger-Liszkay A (2003) Evidence that cytochrome b559 mediates the oxidation of reduced plastoquinone in the dark. J Biol Chem **278:** 13554-13560

Briat JF, Lobreaux S, Grignon N, Vansuyt G (1999) Regulation of plant ferritin synthesis: how and why? Cell Mol Life Sci **56:** 155-166

Carter C, Pan S, Zouhar J, Avila EL, Girke T, Raikhel NV (2004) The vegetative vacuole proteome of *Arabidopsis thaliana* reveals predicted and unexpected proteins. Plant Cell **16:** 3285-3303

Colangelo EP, Guerinot ML (2006) Put the metal to the petal: metal uptake and transport throughout plants. Curr Opin Plant Biol **9:** 322-330

Connolly EL, Fett JP, Guerinot ML (2002) Expression of the IRT1 metal transporter is controlled by metals at the levels of transcript and protein accumulation. Plant Cell **14:** 1347-1357

Curie C, Alonso JM, Le Jean M, Ecker JR, Briat JF (2000) Involvement of NRAMP1 from *Arabidopsis thaliana* in iron transport. Biochem. J. **347:** 749-755

Delhaize E, Gruber BD, Pittman JK, White RG, Leung H, Miao Y, Jiang L, Ryan PR, Richardson AE (2007) A role for the AtMTP11 gene of Arabidopsis in manganese transport and tolerance. Plant J **51:** 198-210

Delhaize E, Kataoka T, Hebb DM, White RG, Ryan PR (2003) Genes encoding proteins of the cation diffusion facilitator family that confer manganese tolerance. Plant Cell **15:** 1131-1142

Dellagi A, Rigault M, Segond D, Roux C, Kraepiel Y, Cellier F, Briat JF, Gaymard F, Expert D (2005) Siderophore-mediated upregulation of Arabidopsis ferritin expression in response to *Erwinia chrysanthemi* infection. Plant J **43:** 262-272

Ducruet JM, Miranda T (1992) Graphical and numerical analysis of thermoluminescence and fluorescence F0 emission in photosynthetic material. Photosynth Res **33:** 15-27

Ferro M, Salvi D, Riviere-Rolland H, Vermat T, Seigneurin-Berny D, Grunwald D, Garin J, Joyard J, Rolland N (2002) Integral membrane proteins of the chloroplast envelope: identification and subcellular localization of new transporters. Proc Natl Acad Sci U S A **99:** 11487-11492

González A, Lynch J (1999) Subcellular and tissue Mn compartmentation in bean leaves under Mn toxicity stress. Aust J Plant Physiol **26:** 811–822

Hebbern CA, Laursen KH, Ladegaard AH, Schmidt SB, Pedas P, Bruhn D, Schjoerring JK, Wulfsohn D, Husted S (2009) Latent manganese deficiency increases transpiration in barley (*Hordeum vulgare*). Physiol Plant **135:** 307-316

Hirschi KD, Korenkov VD, Wilganowski NL, Wagner GJ (2000) Expression of arabidopsis CAX2 in tobacco. Altered metal accumulation and increased manganese tolerance. Plant Physiol **124:** 125-133

Husted S, Laursen KH, Hebbern CA, Schmidt SB, Pedas P, Haldrup A, Jensen PE (2009) Manganese deficiency leads to genotype-specific changes in fluorescence induction kinetics and state transitions. Plant Physiol **150:** 825-833

Ifuku K, Yamamoto Y, Ono TA, Ishihara S, Sato F (2005) PsbP protein, but not PsbQ protein, is essential for the regulation and stabilization of photosystem II in higher plants. Plant Physiol **139:** 1175-1184

Inoue Y (1996) Photosynthetic thermoluminescence as a simple probe of photosystem II electron transport. *In* J Amesz, AJ Hoff, eds, Biophysical techniques in photosynthesis. Kluwer academic publishers, Netherlands, pp 93-107

Kim SA, Punshon T, Lanzirotti A, Li L, Alonso JM, Ecker JR, Kaplan J, Guerinot ML (2006) Localization of iron in Arabidopsis seed requires the vacuolar membrane transporter VIT1. Science **314:** 1295-1298

Koren'kov V, Park S, Cheng NH, Sreevidya C, Lachmansingh J, Morris J, Hirschi K, Wagner GJ (2006) Enhanced Cd^{2+}-selective root-tonoplast-transport in tobaccos expressing Arabidopsis cation exchangers. Planta **225:** 403-411

Korshunova YO, Eide D, Clark WG, Guerinot ML, Pakrasi HB (1999) The IRT1 protein from *Arabidopsis thaliana* is a metal transporter with a broad substrate range. Plant Mol Biol **40:** 37-44

Lanquar V, Lelièvre F, Barbier-Brygoo H, Thomine S (2004) Regulation and function of AtNRAMP4 metal transporter protein. Soil Sci. Plant Nutr. **50:** 1141-1150

Lanquar V, Lelièvre F, Bolte S, Hames C, Alcon C, Neumann D, Vansuyt G, Curie C, Schroder A, Kramer U, Barbier-Brygoo H, Thomine S (2005) Mobilization of vacuolar iron by AtNRAMP3 and AtNRAMP4 is essential for seed germination on low iron. EMBO J **24:** 4041-4051

Liu XF, Culotta VC (1999) Post-translation control of Nramp metal transport in yeast. Role of metal ions and the *BSD2* gene. J. Biol. Chem. **274:** 4863-4868

Long JC, Sommer F, Allen MD, Lu SF, Merchant SS (2008) FER1 and FER2 encoding two ferritin complexes in *Chlamydomonas reinhardtii* chloroplasts are regulated by iron. Genetics **179:** 137-147

Luk EE, Culotta VC (2001) Manganese superoxide dismutase in *Saccharomyces cerevisiae* acquires its metal co-factor through a pathway involving the Nramp metal transporter, Smf2p. J Biol Chem **276:** 47556-47562

Makui H, Roig E, Cole ST, Helmann JD, Gros P, Cellier MF (2000) Identification of the *Escherichia coli* K-12 Nramp orthologue (MntH) as a selective divalent metal ion transporter. Mol. Microbiol. **35:** 1065-1078

Marschner H (1995) Mineral Nutrition of Higher Plants. Academic Press, London

Maxwell K, Johnson GN (2000) Chlorophyll fluorescence--a practical guide. J Exp Bot **51:** 659-668

Mills RF, Doherty ML, Lopez-Marques RL, Weimar T, Dupree P, Palmgren MG, Pittman JK, Williams LE (2008) ECA3, a Golgi-localized P2A-type ATPase, plays a crucial role in manganese nutrition in Arabidopsis. Plant Physiol **146:** 116-128

Nevo Y, Nelson N (2006) The NRAMP family of metal-ion transporters. Biochim Biophys Acta **1763:** 609-620

Oomen RJ, Wu J, Lelièvre F, Blanchet S, Richaud P, Barbier-Brygoo H, Aarts MG, Thomine S (2009) Functional characterization of NRAMP3 and NRAMP4

26

from the metal hyperaccumulator *Thlaspi caerulescens*. New Phytol **181:** 637-650

Patzer SI, Hantke K (2001) Dual repression by Fe^{2+}-Fur and Mn^{2+}-MntR of the mntH gene, encoding an NRAMP-like Mn^{2+} transporter in *Escherichia coli*. J Bacteriol **183:** 4806-4813

Pedas P, Hebbern CA, Schjoerring JK, Holm PE, Husted S (2005) Differential capacity for high-affinity manganese uptake contributes to differences between barley genotypes in tolerance to low manganese availability. Plant Physiol **139:** 1411-1420

Pedas P, Ytting CK, Fuglsang AT, Jahn TP, Schjoerring JK, Husted S (2008) Manganese efficiency in barley: identification and characterization of the metal ion transporter HvIRT1. Plant Physiol **148:** 455-466

Peiter E, Montanini B, Gobert A, Pedas P, Husted S, Maathuis FJ, Blaudez D, Chalot M, Sanders D (2007) A secretory pathway-localized cation diffusion facilitator confers plant manganese tolerance. Proc Natl Acad Sci U S A **104:** 8532-8537

Pittman JK (2005) Managing the manganese: molecular mechanisms of manganese transport and homeostasis. New Phytol **167:** 733-742

Pittman JK, Shigaki T, Marshall JL, Morris JL, Cheng NH, Hirschi KD (2004) Functional and regulatory analysis of the Arabidopsis thaliana CAX2 cation transporter. Plant Mol Biol **56:** 959-971

Portnoy ME, Liu XF, Culotta VC (2000) *Saccharomyces cerevisiae* expresses three functionally distinct homologues of the nramp family of metal transporters. Mol. Cell. Biol. **20:** 7893-7902

Que Q, Helmann JD (2000) Manganese homeostasis in *Bacillus subtilis* is regulated by MntR, a bifunctional regulator related to the diphtheria toxin repressor family of proteins. Mol. Microbiol. **35:** 1454-1468

Quiquampoix H, Loughman BC, Ratcliffe RG (1993) Quantitative Aspects of the ^{31}P-NMR Detection of Manganese in Plant Tissues J. Exp. Bot. **44:** 1809-1818

Ravet K, Touraine B, Boucherez J, Briat JF, Gaymard F, Cellier F (2009a) Ferritins control interaction between iron homeostasis and oxidative stress in Arabidopsis. Plant J **57:** 400-412

Ravet K, Touraine B, Kim SA, Cellier F, Thomine S, Guerinot ML, Briat JF, Gaymard F (2009b) Post-Translational Regulation of AtFER2 Ferritin in Response to Intracellular Iron Trafficking during Fruit Development in Arabidopsis. Mol Plant **2:** 1095-1106

Rutherford AW, Crofts AR, Inoue Y (1982) Thermoluminescence as a probe of photosystem II photochemistry: the origin of the flash-induced glow peaks. Biochim Biophys Acta **682:** 457-465

Sarafian V, Kim Y, Poole RJ, Rea PA (1992) Molecular cloning and sequence of cDNA encoding the pyrophosphate-energized vacuolar membrane proton pump of *Arabidopsis thaliana*. Proc Natl Acad Sci U S A **89:** 1775-1779

Segond D, Dellagi A, Lanquar V, Rigault M, Patrit O, Thomine S, Expert D (2009) NRAMP genes function in *Arabidopsis thaliana* resistance to *Erwinia chrysanthemi* infection. Plant J **58:** 195-207

Seguela M, Briat JF, Vert G, Curie C (2008) Cytokinins Negatively Regulate the Root Iron Uptake Machinery in Arabidopsis through a growth-dependent pathway. Plant J **55:** 289-300

1 **Thomine S, Lelièvre F, Debarbieux E, Schroeder JI, Barbier-Brygoo H** (2003)
2   AtNRAMP3, a multispecific vacuolar metal transporter involved in plant
3   responses to iron deficiency. Plant J. **34:** 685-695
4 **Thomine S, Wang R, Ward JM, Crawford NM, Schroeder JI** (2000) Cadmium and
5   iron transport by members of a plant metal transporter family in *Arabidopsis*
6   with homology to Nramp genes. Proc. Natl. Acad. Sci. USA. **97:** 4991-4996
7 **Vert G, Grotz N, Dedaldechamp F, Gaymard F, Guerinot ML, Briat JF, Curie C**
8   (2002) IRT1, an *Arabidopsis* transporter essential for iron uptake from the soil
9   and for plant growth. Plant Cell **14:** 1223-1233
10 **Wada S, Ishida H, Izumi M, Yoshimoto K, Ohsumi Y, Mae T, Makino A** (2009)
11   Autophagy plays a role in chloroplast degradation during senescence in
12   individually darkened leaves. Plant Physiol **149:** 885-893
13 **White PJ, Bowen HC, Demidchik V, Nichols C, Davies JM** (2002) Genes for
14   calcium-permeable channels in the plasma membrane of plant root cells.
15   Biochim Biophys Acta **1564:** 299-309
16 **Wu Z, Liang F, Hong B, Young JC, Sussman MR, Harper JF, Sze H** (2002) An
17   endoplasmic reticulum-bound Ca^{2+}/Mn^{2+} pump, ECA1, supports plant growth
18   and confers tolerance to Mn^{2+} stress. Plant Physiol **130:** 128-137
19
20
21
22

Figure Legends

Figure 1: AtNRAMP3 and AtNRAMP4 proteins reside on mesophyll vacuoles and are involved in the control of vacuolar Mn content.

(A) Immunoblot analysis of proteins from leaves, mesophyll protoplasts and mesophyll vacuoles from wild-type and *nramp3nramp4* mutant plants. The blots were probed with an anti-NRAMP3, an anti-NRAMP4 antibody or an antibody raised against the vacuolar membrane pyrophosphatase (V-PPase).

(B) Fe, Mn and Zn concentrations in leaves (left), protoplasts (middle) and vacuoles (right) measured by ICP-AES. Grey bars: wild type, white bars: *nramp3nramp4*. Leaf metal concentration is expressed as $\mu g.g^{-1}$; protoplast and vacuole metal contents are expressed as pg per object. Mean ± s.e. $n = 6$ independent experiments for the protoplast preparations; $n = 7$ independent experiments for vacuole. * and *** denote significant differences based on Mann Whitney U-test between genotypes with $p < 0.05$ (*) and $p < 0.001$ (***) respectively.

In A and B, plants were grown on soil for 6 weeks.

Figure 2: Arabidopsis *nramp3nramp4* plants display a growth reduction in the absence of manganese supply in the medium which is rescued by expression of *AtNRAMP3* or *AtNRAMP4* genes.

Plants were grown on perlite for 8 weeks (A, D) or 9.5 weeks (B, C) on control medium (5 μM Mn) or - Mn medium (0 μM Mn). (A) Photographs of wild-type and *nramp3nramp4* rosettes. (B) Leaves of wild type and *nramp3nramp4*. Left: younger leaves; right: older leaves. (C) Fresh biomass of wild-type (WT), *nramp3* (*nr3*), *nramp4* (*nr4*) and *nramp3nramp4* (*nr3nr4*) rosettes. Mean value ± s.e. ($n = 10$-20) plants for each genotype in each condition). (D) Fresh biomass of wild-type (WT), *nramp3nramp4* (*nr3nr4*), *nramp3nramp4 AtNRAMP3* (*nr3nr4*+NR3) and *nramp3nramp4 AtNRAMP4* (*nr3nr4*+NR4) rosettes. Mean value ± s.e. ($n = 12$-24 plants for each genotype in each condition). Different letters denote a statistically significant difference ($p < 0.01$ based on Kruskal Walis test for multiple comparisons).

29

1 **Figure 3**: Mn concentration in leaves and mesophyll protoplasts is equal or higher in

2 *nramp3nramp4* than in wild type.

3 Wild-type (grey bars) or *nramp3nramp4* (white bars) plants were grown on perlite for

4 leaf metal concentration measurements and in hydroponic condition for protoplast

5 relative metal concentrations under control (C: 5 μM Mn) or Mn deficient (- Mn) for 8

6 weeks.

7 (A) Mean ± s.e. of Fe, Mn and Zn concentrations of leaves from plants grown on

8 perlite (*n* = 3 samples containing each 10 leaves from 3-4 plants).

9 (B) Mean ± s.e. of Fe, Mn and Zn relative concentrations of protoplast from plants

10 grown under hydroponic conditions (*n* = 3 protoplast preparations from independent

11 biological replicates). Results are expressed as relative units (R.U.): Fe, Mn and Zn

12 metal content were normalized to the geometric mean of all other reliably measured

13 element contents (Ca, Cu, Fe, Mg, Mn, Mo, P and Zn). Note that expressing the

14 results as metal content / protoplast yielded similar results.

15 Asterisks indicate statistically significant differences between wild type and *nramp3*

16 *nramp4* mutant (Mann Whitney U-test, $p < 0.01$).

17

18 **Figure 4**: PSII activity and chloroplast Mn content are altered in Mn deficient

19 *nramp3nramp4* plants.

20 (A) Intensity of thermoluminescence signals recorded from excised leaf pieces of

21 dark-adapted manganese-deficient wild-type and *nramp3nramp4* plants grown on

22 perlite for 8 weeks under Mn deficient conditions. Black and grey squares represent

23 the amplitude in arbitrary units (a.u.) of the TL (Thermo Luminescence) B band in

24 wild-type and *nramp3nramp4* leaf segments, respectively. Series of zero to eight

25 single turnover flashes were given at 1°C after 5 min of dark adaptation of the leaf

26 segment at 20°C. Similar results were obtained in 2 independent biological

27 replicates.

28 (B) Fluorescence recovery after photoinhibition measured on attached leaves of

29 double mutant (left) and wild-type (right) plants grown on perlite for 8 weeks under

30 Mn deficient conditions. Upper panel: plants grown in the absence of Mn (- Mn),

31 lower panel: plants grown in control conditions (C: 5 μM Mn). Open arrows:

32 onset/termination of the measuring light; closed arrows: onset/termination of the

33 actinic light (white light at 2000 μmol quanta $m^{-2}s^{-1}$); dim light (6 μmol quanta $m^{-2}s^{-1}$).

34 Similar results were obtained in 2 independent biological replicates.

(C) D1 (PsbA) protein levels in leaves of wild-type or *nramp3nramp4* plants analyzed by immunoblot (higher panel). Five, 2.5, 1.25 and 0.62 μg total leaf proteins from 9.5 week old plants grown on perlite under control (C: 5 μM Mn) or Mn deficient (- Mn) conditions were loaded. Silver staining of proteins on gels run in parallel indicate that equal amounts of proteins were loaded (lower panel). Similar results were obtained in 3 independent biological replicates.

(D) Relative Mn concentrations of intact chloroplasts isolated from wild-type (grey bars) or *nramp3nramp4* (white bars) plants grown under control (C: 5 μM Mn) or Mn deficient (- Mn) for 8 weeks in hydroponic conditions. Mn concentrations were normalized to the geometric mean of all other reliably measured element concentrations (Cu, P and S). Note that additional elements could not be used for normalization because of their concentrations in the chloroplast suspension buffer. Results are expressed as mean ratio ± s.e. taking the Mn content in chloroplast from wild-type plants grown under control conditions as reference (n = 3 independent biological replicates).

Figure 5: MnSOD activity is maintained in *nramp3nramp4* Mn deficient leaves.

In-gel SOD activity staining was performed in the absence (A) or in the presence of 5 mM H_2O_2 (B). Hundred micrograms of total leaf proteins from 9.5 week old plants grown on perlite under control (C: 5 μM Mn), Fe deficient (- Fe) or Mn deficient (- Mn) were separated by native PAGE before activity staining. Similar results were obtained with 2 independent biological replicates.

Figure 6: AtNRAMP3 and AtNRAMP4 protein levels are not regulated in response to Mn deficiency but ferritins are accumulated in shoots of Mn-deficient *nramp3nramp4* plants.

(A) AtNRAMP3 and AtNRAMP4 protein levels in roots and shoots of wild-type plants analyzed by immunoblot. Extracts of root and shoot proteins from *nramp3nramp4* plants grown on control medium were loaded as a negative control.

(B) Ferritin and IRT1 protein levels were monitored by immunoblot on *nramp3nramp4* and wild-type plants. The FER1 antibody was used on blots of shoot extracts and the IRT1 antibody was used on blots of root extracts.

In A and B, 15 µg total proteins from roots or shoots of plants grown for 6 weeks under hydroponic conditions were analyzed. Mn deficient plants were grown without added Mn in the growth medium for 6 weeks. To induce Fe deficiency, after 4 weeks, plants were transferred in a medium containing 20 µM Ferrozine in the absence of added Fe for 2 more weeks.

1

2

3 **Table I**: Rosette fresh biomass and chlorophyll fluorescence of 8-week-old wild-type

4 and *nramp3nramp4* plants grown on perlite in presence (control: 5 µM Mn) or

5 absence of manganese (- Mn). Results shown correspond to mean ± s.e. with *n*

6 number of plants weighted and *n'* number of Fv/Fm measurements on different

7 leaves. Results from one representative experiment out of 5. Mann-Whitney U-test,

8 **$p < 0.01$, *$p < 0.05$, $^{\triangle}p > 0.05$.

9

	Fresh biomass (*n*)	Fv/Fm (*n'*)
Control medium		
Wild type	537 ± 69 (11)	0.798 ± 0.003 (10)
nramp3nramp4	582 ± 92$^{\Delta}$ (6)	0.796 ± 0.004 $^{\Delta}$ (12)
- Mn medium		
Wild type	279 ± 36 (15)	0.655 ± 0.013 (11)
nramp3nramp4	82 ± 24** (10)	0.572 ± 0.017* (9)

10

11

12

13
14
15
16
17
18
19
20

33

A

| | nramp3 nramp4 | Wild type | nramp3 nramp4 | Wild type | nramp3 nramp4 | Wild type |

NRAMP3

NRAMP4

V-PPase

Leaves — Protoplasts from mesophyll — Vacuoles from mesophyll

B

Leaves

Protoplasts from mesophyll

Vacuoles from mesophyll

Metal concentration (µg/g leaf DW)

Metal concentration (pg/ protoplast)

Metal concentration (pg / vacuole)

Fe Mn Zn

Fe Mn Zn

Fe Mn Zn

Figure 1
Lanquar *et al*

A

Wild type

nramp3nramp4

Wild type

nramp3nramp4

C

- Mn

B

Wild type

nramp3nramp4

C

Wild type

nramp3nramp4

- Mn

C

Fresh biomass (mg.plant⁻¹)

legend: WT, nr3, nr4, nr3nr4

D

Fresh biomass (mg.plant⁻¹)

legend: WT, nr3nr4, nr3nr4+NR3, nr3nr4+NR4

Figure 2
Lanquar *et al*

Figure 3
Lanquar *et al*

A

TL intensity (a.u.)

Number of flashes

B

nramp3nramp4 - Mn

Wild type - Mn

nramp3nramp4 C

Wild type C

1h light · 3h dim light

1h light · 3h dim light

C

kDa

Wild type

nramp3nramp4

37 —

— C

37 —

25 —

— Mn

5 · 2.5 · 1.25 · 0.625 µg

25 —

— C

25 —

— Mn

D

Relative chloroplast Mn concentration

WT
nr3nr4

C

- Mn

Figure 4

Lanquar *et al*

A

Wild type   *nramp3nramp4*

C   - Fe   - Mn   C   - Fe   - Mn

MnSOD ▶
FeSOD ▶

CuZnSOD ▶

B

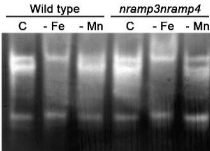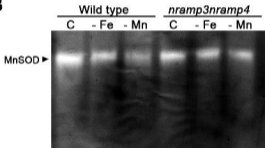Wild type   *nramp3nramp4*

C   - Fe   - Mn   C   - Fe   - Mn

MnSOD ▶

Figure 5
Lanquar *et al*

Figure 6
Lanquar *et al*